

## AN ENERGETIC MAGNETAR IN HESS J1713–381/CTB 37B

J. P. HALPERN AND E. V. GOTTHELF

Columbia Astrophysics Laboratory, Columbia University, 550 West 120th Street, New York, NY 10027-6601, USA;  
jules@astro.columbia.edu, eric@astro.columbia.edu

## ABSTRACT

We obtained a second *Chandra* timing measurement of the 3.82 s pulsar CXOU J171405.7–381031 in the supernova remnant (SNR) CTB 37B, which shows that it is spinning down rapidly. The average period derivative of  $(5.88 \pm 0.08) \times 10^{-11}$  over the 1 year time span corresponds to a dipole magnetic field strength  $B_s = 4.8 \times 10^{14}$  G, well into the magnetar range. The spin-down power  $\dot{E} = 4.2 \times 10^{34}$  erg s<sup>−1</sup> is among the largest for magnetars, and the corresponding characteristic age  $\tau_c \equiv P/2\dot{P} = 1030$  years is comparable to estimates of the age of the SNR. The period derivative enables us to recover probable pulsations in an *ASCA* observation taken in 1996, which yields a mean characteristic age of 860 years over the longer 13 year time span. The source is well detected up to 10 keV, and its composite spectrum is typical of a magnetar. CTB 37B hosts HESS J1713–381, the first TeV source that is coincident with a magnetar. While the TeV emission has been attributed to the SNR shell, it is possibly centrally peaked, and we hypothesize that this particularly young, energetic magnetar may contribute to the HESS source. We also searched for pulsations from another source in a HESS SNR, XMMU J173203.3–344518 in HESS J1731–347/G353.6–0.7, but could not confirm pulsations or long-term flux variability, making it more likely that this source is a weakly magnetized central compact object.

*Subject headings:* ISM: individual (CTB 37B, G353.6–0.7) — pulsars: individual (CXOU J171405.7–381031, XMMU J173203.3–344518) — stars: neutron

## 1. INTRODUCTION

Of the  $\approx 60$  Galactic TeV sources<sup>1</sup>, the majority (43) are identified as either pulsar wind nebulae (PWNe) or supernova remnants (SNRs). The PWN class comprises  $\approx 27$ –30 of these, and it is likely that some of the unclassified sources will also prove to be PWNe. Most pulsars that are responsible for the PWNe detected at X-ray and TeV energies have spin-down power  $\dot{E} \equiv 4\pi^2 I \dot{P}/P^3 > 10^{36}$  erg s<sup>−1</sup>. In Figure 1 we display the distribution of  $\dot{E}$  for rotation-powered pulsars powering TeV nebulae. For reviews of these, see Carrigan et al. (2008), Gallant et al. (2008), Lemi re et al. (2008), Hessels et al. (2008), Mattana et al. (2009), & Kargaltsev & Pavlov (2010). In the standard model of nonthermal emission from PWNe, the X-rays are synchrotron from relativistic electrons and positrons, while the TeV  $\gamma$ -rays are inverse Compton scattered microwave background and other ambient photons from the same population of relativistic particles (e.g., de Jager & Djannati-Ata i 2008; Zhang 2008). In contrast, there is scant evidence that any of the 17 known magnetars<sup>2</sup>, with periods in the range 2–12 s, produce X-ray or TeV PWNe. Including both anomalous X-ray pulsars (AXPs) and soft gamma-ray repeaters (SGRs), the spin-down power of magnetars is  $< 10^{36}$  erg s<sup>−1</sup>, as also plotted in Figure 1. Because of their larger magnetic field strengths and different emission mechanisms from ordinary spin-powered pulsars, it is not predicted that magnetars accelerate par-

ticles to TeV energies (Beloborodov & Thompson 2007; Thompson 2008a,b), except perhaps in their earliest stage of rapid spin-down (Arons 2003).

Halpern & Gotthelf (2010a, hereafter Paper I) presented a study of point X-ray sources in two SNRs detected at TeV energies by the HESS array of atmospheric Cherenkov telescopes. The first of these, HESS J1713–381 associated with CTB 37B, was discovered by Aharonian et al. (2006). Using a *Chandra* observation, Aharonian et al. (2008a) then found the point X-ray source CXOU J171405.7–381031 in CTB 37B, and considered that it could be a pulsar, albeit with an unusually soft, non-thermal spectrum. Nakamura et al. (2009) analyzed *Chandra* and *Suzaku* spectra of CXOU J171405.7–381031, noting possible variability in flux, which they took to be good evidence that it is an anomalous X-ray pulsar (AXP). In Paper I, we reported the discovery of pulsations from CXOU J171405.7–381031 that verifies this conjecture. In Section 2 of this paper, we report a follow-up *Chandra* observation that measures the period derivative of the pulsar, establishing its quantitative magnetar properties.<sup>3</sup> We raise in Section 3 the possibility that at an early stage, a magnetar such as the one in CTB 37B may produce a TeV PWN. In Section 4 we report on a new observation of the second compact X-ray source discussed in Paper I, XMMU J173203.3–344518 in HESS J1731–347/G353.6–0.7, in which pulsations are not confirmed.

<sup>1</sup> VHE  $\gamma$ -ray Sky Map and Source Catalog, <http://www.mppmu.mpg.de/~rwagner/sources/index.html>  
<sup>2</sup> SGR/AXP Online Catalog, <http://www.physics.mcgill.ca/~pulsar/magnetar/main.html>

<sup>3</sup> While this paper was in preparation, the same result was announced by Sato et al. (2010) using an *XMM-Newton* observation.

TABLE 1  
LOG OF TIMING OBSERVATIONS OF CXOU J171405.7–381031 IN CTB 37B

Instrument/Mode	ObsID	Date (UT)	Date (MJD)	Exp. (s)	Counts (s <sup>-1</sup> )	Period (s)
<i>ASCA</i> GIS	54002030	1996 Sep 12	50,338.8	13,322	0.053	3.7954(1)
<i>Chandra</i> ACIS-S3/CC/F	10113	2009 Jan 25	54,856.3	30,146	0.106	3.823056(18)
<i>Chandra</i> ACIS-S3/CC/F	11233	2010 Jan 30	55,226.5	30,124	0.122	3.824936(17)
<i>XMM-Newton</i> EPIC pn	0606020101	2010 Mar 17	55,272.2	40,264	0.264	3.825352(4) <sup>a</sup>

<sup>a</sup> From Sato et al. (2010).

## 2. X-RAY OBSERVATIONS OF CXOU J171405.7–381031 IN HESS J1713–381/CTB 37B

We obtained a new *Chandra* observation of CXOU J171405.7–381031 on 2010 January 30 using the same instrumental setup as our previous observation of 2009 January 25 (Paper I). Both data sets were acquired using the Advanced Camera for Imaging and Spectroscopy (ACIS) in continuous-clocking (CC) mode with the pulsar located on the ACIS-S3 CCD. This provides a time resolution of 2.85 ms and avoids any spectral pile-up. The photon arrival times in CC mode are adjusted in the standard processing to account for the known position of the pulsar, spacecraft dither, and SIM offset. Reduction and analysis used the standard software packages CIAO (v4.1) and CALDB (v3.5.0). A log of the *Chandra* timing observations is given in Table 1.

With a period derivative derived from the *Chandra* observations (see below), we also searched for and likely detected pulsations in archival data taken with the *ASCA* X-ray telescope (Tanaka et al. 1994). The pulsar was imaged with the Gas Imaging Spectrometer (GIS) on 1996 September 12 as part of the Galactic Survey (Sugizaki et al. 2001). It fell on the very edge of the GIS

field of view of sequence #54002030, 21' from the pointing direction, partially in the area masked out by the standard processing. To maximize the sensitivity to the expected pulsar signal, we combined unmasked and unfiltered data taken in low- and high-bit-rate data modes, with timing resolution of 0.5 s and 0.0625 s, respectively. We obtained a total of 712 counts (0.5–10 keV) from the source in a 3' radius aperture during 13.3 ks of usable exposure from the 21 ks observation.

### 2.1. Timing Analysis

The photon arrival times were corrected to the solar system barycenter using the pulsar position obtained from the *Chandra* ACIS-I image. Timing analysis of the *Chandra* data was then performed in an identical manner

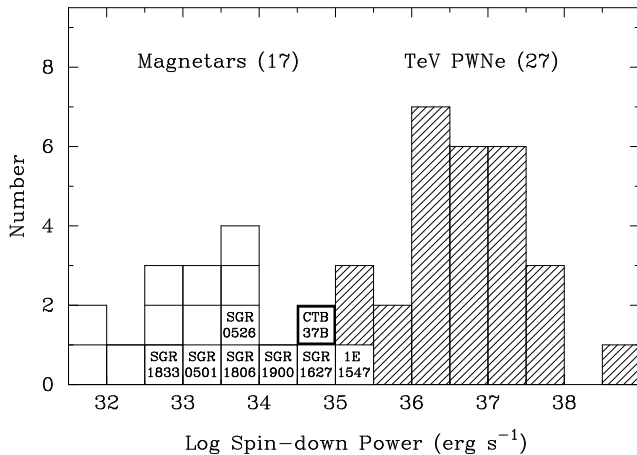


FIG. 1.— Spin-down power of 27 pulsars (hatched) whose PWNe are identified as TeV sources by HEGRA, HESS, VERITAS, MAGIC, and Milagro, in comparison with spin-down power of 17 magnetars (open squares) with measured period derivatives. The TeV PWNe are drawn from the reviews referenced in Section 1, and magnetars from references in Footnote 2. Magnetars that have had SGR outbursts, including 1E 1547.0–5408, are labeled individually; the unlabeled squares are AXPs. The spin-down power of CXOU J171405.7–381031 in CTB 37B is among the largest of magnetars, and falls in the range occupied exclusively by SGRs, although it is not known to be an SGR.

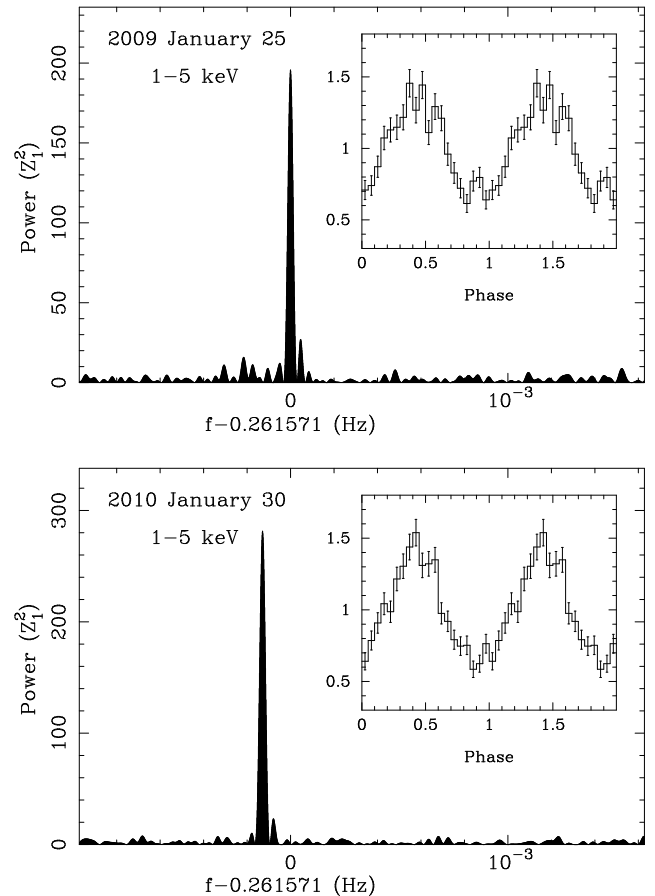


FIG. 2.—  $Z^2$  power spectra of CXOU J171405.7–381031 from the *Chandra* CC-mode observations separated by 1 year, and corresponding folded light curves (inset). Normalized count rate is plotted. Phase is shifted arbitrarily. Note the highly significant decrease in frequency.

TABLE 2  
*Chandra* MEASURED SPIN PARAMETERS OF  
CXOU J171405.7–381031 IN CTB 37B

Parameter	Value
R.A. (J2000) <sup>a</sup>	17 <sup>h</sup> 14 <sup>m</sup> 05 <sup>s</sup> .74
Decl. (J2000) <sup>a</sup>	−38°10′30″.9
Epoch (MJD)	55226.5
Spin period, $P$	3.824936(17) s
Period derivative, $\dot{P}$	$(5.88 \pm 0.08) \times 10^{-11}$
Range of dates (MJD)	54856–55227
Surface dipole magnetic field, $B_s$	$4.8 \times 10^{14}$ G
Spin-down power, $\dot{E}$	$4.2 \times 10^{34}$ erg s <sup>−1</sup>
Characteristic age, $\tau_c$	1030 yr

<sup>a</sup> Measured from *Chandra* ACIS-I ObsID 6692. Typical *Chandra* ACIS coordinate uncertainty is 0′′6.

to Paper I. Photons from the central four source columns (2′′) in the range 1–5 keV, which contains most of the photons, were extracted and searched for pulsations using the Rayleigh test (Strutt 1880), also known as  $Z_1^2$  (Buccheri et al. 1983). The power-spectrum and folded pulse profiles from the two *Chandra* timing observations are shown in Figure 2. Although the eye may be drawn to subtle differences, a  $\chi^2$  test on the difference profile indicates that the two light curves are not significantly different:  $\chi_\nu^2 = 1.44$  for 20 degrees of freedom, corresponding to 9% chance probability. The pulsed fraction is  $f_p \approx 0.38$ , defined as the fraction of counts above the minimum in the light curve, corrected for background. There is no evidence for energy dependence of the pulse profile. While it is possible that the true period is 7.6 s, with two peaks per rotation, there is no strong evidence to support this in the form of distinguishable peaks in the current data.

The periods and  $1\sigma$  uncertainties for the two *Chandra* observations are listed in Table 1, while the period derivative listed in Table 2 is calculated from the difference between the periods measured 1 year apart. The uncertainty on  $\dot{P}$  is propagated from the statistical errors in the individual period measurements. The  $\dot{P} = (5.88 \pm 0.08) \times 10^{-11}$  over the 1 year time span corresponds to a dipole magnetic field strength  $B_s = 3.2 \times 10^{19} (P\dot{P})^{1/2} = 4.8 \times 10^{14}$  G, well into the magnetar range. The spin-down power  $\dot{E} = 4.2 \times 10^{34}$  erg s<sup>−1</sup> is among the largest for magnetars, and the characteristic age  $\tau_c \equiv P/2\dot{P} = 1030$  years is among the smallest.

A third period measurement was obtained by Sato et al. (2010) using *XMM-Newton*, only 47 days after our second *Chandra* timing observation. They reported  $P = 3.825352 \pm 0.000004$  s on 2010 March 17–18. As shown in Figure 3, this third point requires a significant increase in  $\dot{P}$  to  $1.05 \times 10^{-10}$ . Such variation is common in magnetars, and in this case may indicate that the spin-down power was recently as large as  $\approx 7 \times 10^{34}$  erg s<sup>−1</sup>.

We recovered a fourth period measurement from the archival *ASCA* observation listed in Table 1 by extrapolating the *Chandra* ephemeris. This detection shown in Figure 4, while not significant in a blind search, has a false detection probability of only  $1.1 \times 10^{-3}$  when the search is restricted to a range of  $\dot{P}$  up to twice the *Chandra* measured value. The implied period deriva-

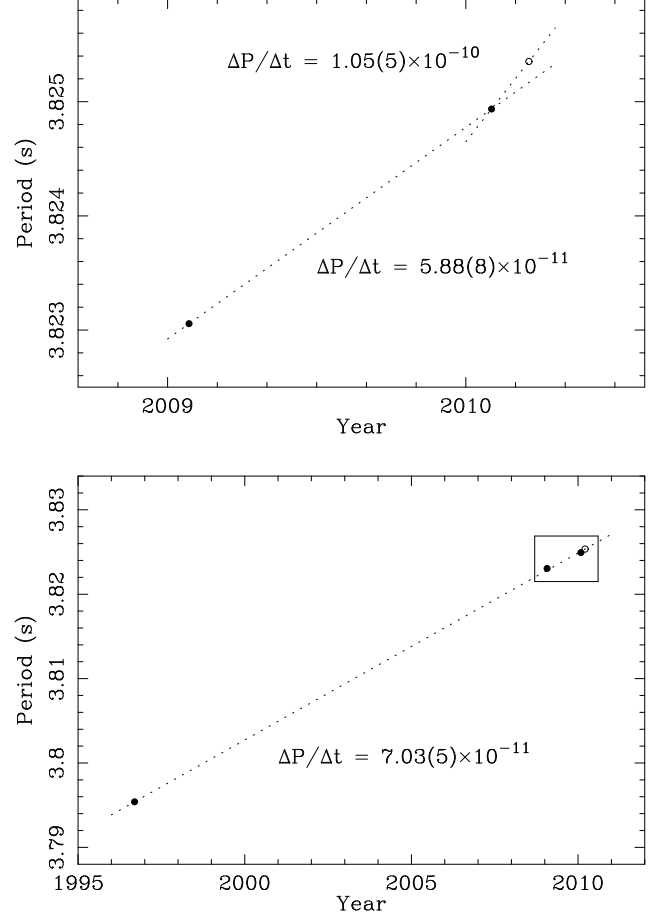


FIG. 3.— (Top) Period measurements of CXOU J171405.7–381031 from the two *Chandra* CC-mode observations (filled circles) and the one *XMM-Newton* observation (Stato et al. 2010, open circle). Error bars are smaller than the size of the symbols. Period derivatives between consecutive measurements are indicated. A significant increase in  $\dot{P}$  is seen. (Bottom) Average period derivative from 1996 to 2010 when including the probable *ASCA* GIS detection in 1996. The box encloses the range of the top panel.

tive relative to the 2009 *Chandra* measurement is  $\dot{P} = 7.08 \times 10^{-11}$ , and the strength of the highly modulated signal is plausible. As shown in Figure 4, which includes an extended range of period derivatives up to 10 times the *Chandra* value, no other significant peak is found. Figure 3 shows the average  $\dot{P}$  obtained in an unweighted fit to all four existing period measurements,  $\dot{P} = 7.03 \times 10^{-11}$  corresponding to  $\tau_c = 860$  years, very close to the *Chandra* measured values, but perhaps a better representation of the long-term average. Keeping in mind that  $\dot{P}$  is evidently variable, the ephemeris in Table 2 includes only the two *Chandra* points, which present the minimum observed value of  $\dot{P}$ .

## 2.2. Spectral Analysis

Spectral data for the pulsar were extracted from the *Chandra* CC-mode observations using the five central source columns, corresponding to a diameter of 2′′46 and  $\approx 95\%$  of the point-source energy enclosed. The background for the spectrum was obtained from the regions adjacent to the source. Background subtracted count

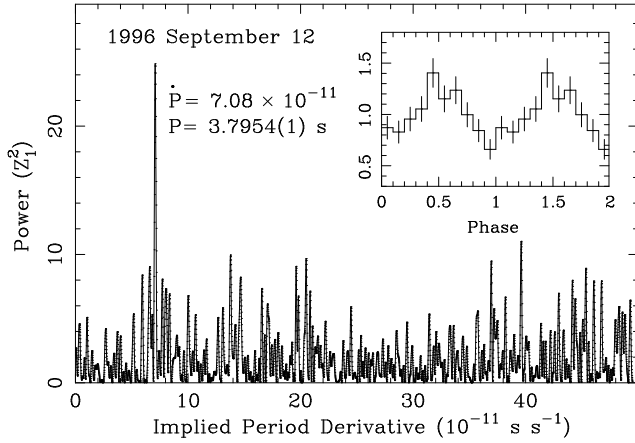


FIG. 4.— Period search of CXOU J171405.7–381031 in the *ASCA* GIS observation of 1996 September 12. Period is converted to the  $\dot{P}$  needed to extrapolate from the *Chandra* observation of 2009. Inset: Folded light curve in the total (0.5–10 keV) energy band corresponding to the indicated highest peak in the power spectrum. Normalized count rate is plotted.

rates are  $0.106 \pm 0.002$  and  $0.122 \pm 0.002$  s $^{-1}$ , respectively, for the two observations, indicating a likely change of  $\approx 15\%$ .

The standard spectral response matrices were generated for the target location on the CCD using the CIAO tool `psextract`, with care taken to normalize the background according to area. All spectra were corrected for the effects of charge-transfer inefficiency; however, the spectral gain is not calibrated well in CC mode. The resulting spectra were grouped with a minimum of 50 counts per bin and fitted using the XSPEC software Arnaud (1996) to power-law, two blackbody, and Comptonized blackbody models. The spectral fits are shown in Figure 5, and the best fitted parameters for these models are listed in Table 3. A single blackbody model does not yield a good fit, and is not shown.

In paper I the ACIS-I/TE mode observation of 2007 indicated a rising spectrum above 6 keV, but the CC-mode spectra presented here do not clearly show that property. We suspect that the previous spectrum may have suffered systematic effects as the pulsar was dithered into the gap between CCDs. In addition, a small amount of spectral pileup in TE mode is avoided in CC mode. Nevertheless, the source is definitely detected up to 10 keV, and shows some evidence for an upturn there in the slightly brighter state of 2010.

### 3. DISCUSSION

#### 3.1. CXOU J171405.7–381031 as a Magnetar

The *Chandra* CC-mode spectra of CXOU J171405.7–381031 are fitted equally well by power-law, two blackbody, and Comptonized blackbody models. Of these, we disfavor the steep  $\Gamma \approx 4.2$  power-law model as being least plausible on physical grounds. In the thermal models, there is a blackbody component of temperature  $\approx 0.4$  keV that covers  $\approx 10\%$  of the surface area of the neutron star. A harder component is also needed that can be parameterized as either a second blackbody or a power-law tail, the latter approximating what is probably cyclotron resonance scattering (Fernández & Thompson 2007) using a simpli-

TABLE 3  
*Chandra* SPECTRAL FITS FOR CXOU J171405.7–381031 IN CTB 37B

Parameter	2009 Jan 25	2010 Jan 30
<b>Power-Law Model</b>		
$N_{\text{H}}$ ( $10^{22}$ cm $^{-2}$ )	$5.46 \pm 0.36$	$5.36 \pm 0.34$
$\Gamma$	$4.25 \pm 0.23$	$4.12 \pm 0.22$
$F_x$ (2 – 10 keV) <sup>a</sup>	$1.26 \times 10^{-12}$	$1.48 \times 10^{-12}$
$L_x$ (2 – 10 keV) <sup>b</sup>	$2.4 \times 10^{34}$	$2.7 \times 10^{34}$
$\chi^2_{\nu}$	1.06(56)	1.07(67)
<b>Two Blackbody Model</b>		
$N_{\text{H}}$ ( $10^{22}$ cm $^{-2}$ )	$3.81^{+0.44}_{-0.27}$	$4.01^{+0.67}_{-0.28}$
$kT_1$ (keV)	$0.45^{+0.02}_{-0.08}$	$0.43^{+0.03}_{-0.08}$
$R_1$ (km)	$2.6^{+3.1}_{-0.9}$	$3.2^{+3.9}_{-1.2}$
$kT_2$ (keV)	$1.13^{+0.48}_{-0.27}$	$1.13^{+0.38}_{-0.23}$
$R_2$ (km)	$0.19^{+0.32}_{-0.13}$	$0.22^{+0.28}_{-0.14}$
$F_x$ (2 – 10 keV) <sup>a</sup>	$1.28 \times 10^{-12}$	$1.50 \times 10^{-12}$
$L_x$ (2 – 10 keV) <sup>b</sup>	$1.8 \times 10^{34}$	$2.2 \times 10^{34}$
$L_{\text{bol}}$ <sup>b</sup>	$4.2 \times 10^{34}$	$5.4 \times 10^{34}$
$\chi^2_{\nu}$	1.11(54)	1.07(65)
<b>Comptonized Blackbody Model</b>		
$N_{\text{H}}$ ( $10^{22}$ cm $^{-2}$ )	$4.12^{+0.50}_{-0.41}$	$4.11^{+0.82}_{-0.34}$
$kT$ (keV)	$0.38^{+0.08}_{-0.05}$	$0.38^{+0.08}_{-0.05}$
$R$ (km)	$3.3^{+3.4}_{-1.6}$	$3.5^{+9.0}_{-1.3}$
$\Gamma$	$3.34^{+0.18}_{-0.20}$	$3.22^{+0.32}_{-0.15}$
$F_x$ (2 – 10 keV) <sup>a</sup>	$1.32 \times 10^{-12}$	$1.57 \times 10^{-12}$
$L_x$ (2 – 10 keV) <sup>b</sup>	$1.8 \times 10^{34}$	$2.2 \times 10^{34}$
$\chi^2_{\nu}$	1.10(55)	1.04(66)

<sup>a</sup> Absorbed flux in units of erg cm $^{-2}$  s $^{-1}$ .

<sup>b</sup> Unabsorbed luminosity in units of erg s $^{-1}$ , assuming  $d = 8$  kpc.

fied analytic expression in the Comptonized blackbody model (Halpern et al. 2008, and references therein). The hot spot(s), and possibly anisotropic scattering in the magnetosphere, are responsible for the observed pulsations, although there is no obvious dependence of the pulse shape on energy. In either the two blackbody or the Comptonized blackbody model, the associated  $N_{\text{H}} \approx 4 \times 10^{22}$  cm $^{-2}$  is compatible with its value in fits to the thermal emission from the SNR (Nakamura et al. 2009), which yield  $N_{\text{H}} = 3.5^{+0.5}_{-0.7} \times 10^{22}$  cm $^{-2}$ . This provides some additional support for the association of CXOU J171405.7–381031 with CTB 37B.

Other properties of CXOU J171405.7–381031 are consistent with those of AXPs: a factor of  $\approx 1.8$  flux decrease is reported between the earlier *Suzaku* and *Chandra* observations (Nakamura et al. 2009). The spin-down power of CXOU J171405.7–381031,  $\dot{E} \geq 4.2 \times 10^{34}$  erg s $^{-1}$ , is among the highest for magnetars, exceeded only by SGR/AXP 1E 1547.0–5408 ( $\dot{E} \geq 1 \times 10^{35}$  erg s $^{-1}$ ; Camilo et al. 2007, 2008), and equalled by SGR 1627–41 ( $\dot{E} = 4.3 \times 10^{34}$  erg s $^{-1}$ ; Esposito et al. 2009) and SGR 1806–20 when in its active state,  $\dot{E} \sim 5 \times 10^{34}$  erg s $^{-1}$ , although here we adopt a more typical quiescent value of  $8 \times 10^{33}$  erg s $^{-1}$  (Woods et al. 2007). The range of  $\dot{E}$  in which CXOU J171405.7–381031 falls (Figure 1) is occupied by SGRs rather than AXPs. By analogy with the history of 1E 1547.0–5408 and other high- $\dot{E}$  magnetars that exhibit large fluctuations in  $\dot{P}$ , we speculate that CXOU J171405.7–381031 is prone to having SGR outbursts. It also shares with 1E 1547.0–5408 the property that its spin-down power is greater than its X-ray

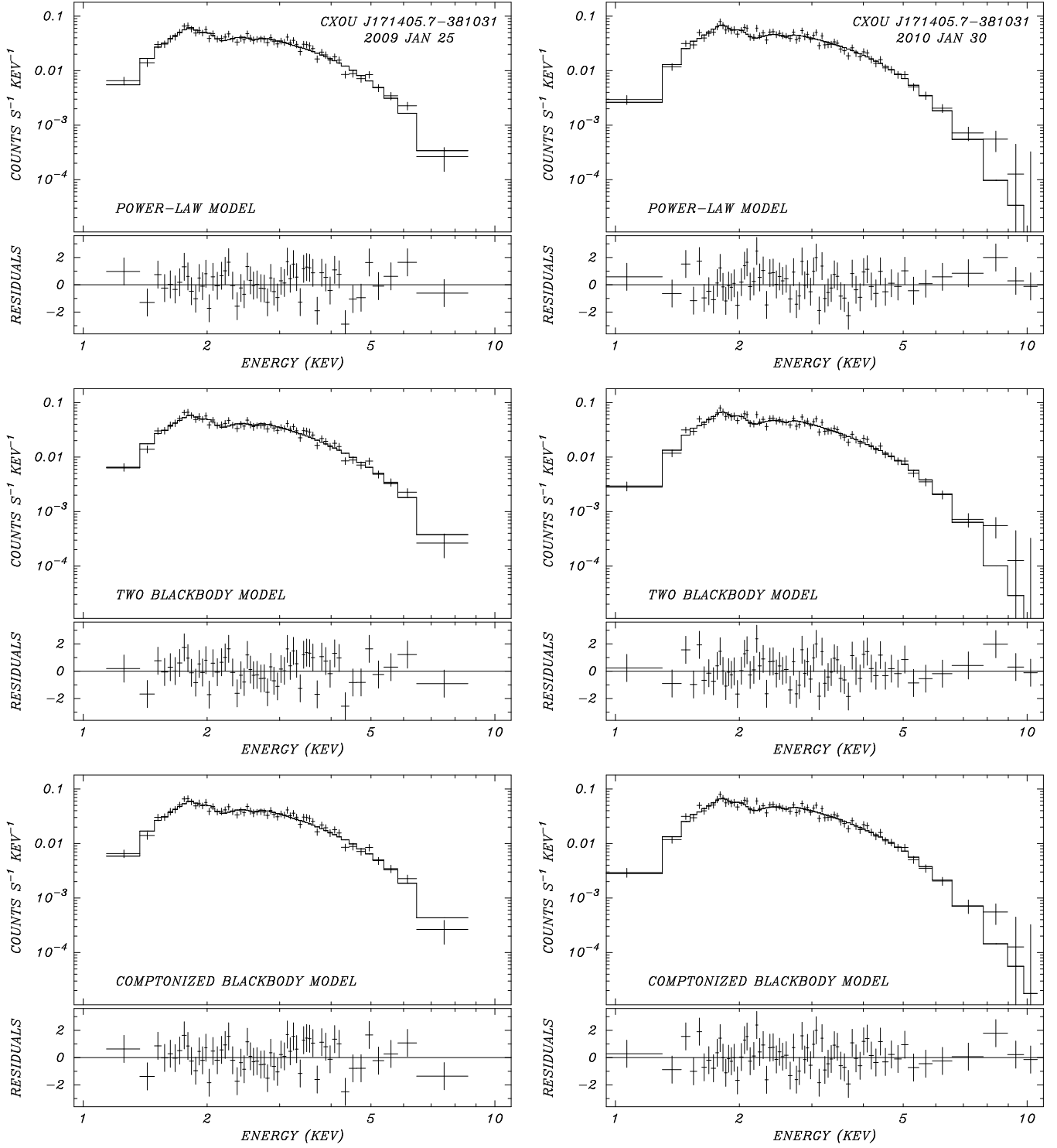


FIG. 5.— Spectra of CXOU J171405.7-381031 in CTB 37B from the *Chandra* ACIS-S3 CC-mode observations of 2009 (left) and 2010 (right) fitted to power-law (top), two blackbody (middle), and Comptonized blackbody models (bottom). Fitted parameters are listed in Table 3.

luminosity ( $L_x \approx 2 \times 10^{34} \text{ erg s}^{-1}$ ), at least in quiescence. However, this does not change our assessment that the majority of its luminosity is generated by magnetic field decay and not by rotation, given its high surface dipole field strength,  $B_s = 4.8 \times 10^{14} \text{ G}$ , X-ray spectral properties, and variability that are typical of magnetars.

### 3.2. Comparison of Age Estimates

At radio wavelengths, CTB 37B is a shell  $\approx 10'$  in diameter (Kassim et al. 1991). Its distance, estimated from H I absorption and the Galactic rotation curve, is  $\approx 8 \text{ kpc}$  (Green 2009). Estimates of the age of CTB 37B are quite varied, and it is of great interest to compare these with the spin-down age of CXOU J171405.7–381031, even though characteristic ages of magnetars are not reliable because their period derivatives are known to vary by a factor of a few.

Clark & Stephenson (1975) tentatively associated CTB 37B with the historical supernova of 393 AD, which would make it 1600 years old, almost twice the pulsar’s characteristic age of  $\sim 860$  years. However, in the same region of the sky the more recently discovered SNR RXJ 1713.7–3946 is a much better candidate for SN 393, as argued by Wang et al. (1997), Wang (2006), and Cassam-Chenaï et al. (2004). At  $d \approx 1.3 \text{ kpc}$  and with  $N_H \approx 5 \times 10^{21} \text{ cm}^{-2}$  (Cassam-Chenaï et al. 2004), RXJ 1713.7–3946 is closer, and an order of magnitude less absorbed than CTB 37B, while the latter is too far away to have been visible for 8 months as the Chinese records indicate. Given this better alternative, we do not regard the birth of CXOU J171405.7–381031 as having been established by historical records. Instead, we turn to estimates of the SNR age from analyses of its thermal X-ray spectrum.

Using the *Chandra* data, Aharonian et al. (2008a) fitted a non-equilibrium ionization model and obtained a Sedov age of  $\approx 4900 \text{ yr}$  for CTB 37B assuming electron-ion equilibrium, while noting that this condition is usually not obtained in young SNRs. Both a higher ion temperature and efficient cosmic ray acceleration have the effect of decreasing the inferred age, perhaps to  $\sim 2700 \text{ yr}$  in the estimate of Aharonian et al. (2008a). Nakamura et al. (2009) then analyzed the *Suzaku* spectrum of CTB 37B and estimated the age of the plasma as  $650_{-300}^{+2500}$  years in the brightest part of the remnant, which also required a relatively low ISM density of  $n_H \sim 0.4 \text{ cm}^{-3}$ . In addition, they found a region of non-thermal power-law emission and a smaller ambient density in the southern part of the SNR. Thus, the SNR age estimate is broadly consistent with the pulsar’s characteristic age, although the uncertainties in both values are large, and their applicability can be questioned.

### 3.3. Magnetar/SNR Associations

Three magnetars are securely associated with shell SNRs because of their central locations: 1E 2259+586 in CTB 109, 1E 1841–045 in Kes 73, SGR 0526–66 in the LMC SNR N49 (Gaensler et al. 2001). To these we may tentatively add 1E 1547.0–5408 because of its possible radio shell G327.24–0.13 (Gelfand & Gaensler 2007), and now CXOU J171405.7–381031 in CTB 37B. In addition to constraining ages for modelling of PWNe, such associations are valuable for inferring natal properties

such as magnetar kick velocity, and possible contribution of an assumed rapidly spinning proto-magnetar to the energetics of the SNR expansion (e.g., Vink & Kuiper 2006). Theories for the birth of magnetars require short initial spin periods, of order a few milliseconds, in order to create their strong  $B$ -fields from a turbulent dynamo whose strength depends on the rotation rate of the proto-neutron star (Thompson & Duncan 1993).

The radio emitting AXP XTE J1810–197 is the only magnetar with a directly measured proper motion, corresponding to  $v_t = 212 \pm 35 \text{ d}_{3.5} \text{ km s}^{-1}$  (Helfand et al. 2007), a value which is not unusual compared to ordinary young neutron stars. Aharonian et al. (2008a) noted that the displacement of CXOU J171405.7–381031 from the center of the shell of CTB 37B would require a transverse velocity of  $\sim 1000 \text{ km s}^{-1}$  for an age of 5000 yr. The velocity would be unreasonably larger if the pulsar characteristic age of  $\sim 1000$  years is adopted as its true age. However, Aharonian et al. (2008a) and Nakamura et al. (2009) also noted that the brighter X-ray and radio emission on the eastern side of the remnant (see Figure 1 of Paper I) is probably due to a higher density there, implying that the pulsar may still be close to the explosion center, which is not the geometric center, reducing its inferred velocity.

Because of this non-uniformity in shock radius  $r_s$  and ISM density  $\rho_0$ , it is difficult to use the standard Sedov evolution

$$r_s^5(t) = \frac{2.026 \mathcal{E}_0 t^2}{\rho_0}$$

as did Vink & Kuiper (2006) for other SNRs hosting magnetars, to estimate the energy  $\mathcal{E}_0$  of the explosion. The radius, which enters to the fifth power, is uncertain by at least a factor of 2. Nevertheless, if we use the values adopted by Nakamura et al. (2009) for the radius, age, and ambient density in the brightest part of the remnant (their region 1), an unremarkable energy of  $\mathcal{E}_0 \sim 1 \times 10^{50} \text{ erg}$  results. Energetic input to the SNR expansion from a presumed millisecond magnetar spinning down is therefore not evident, as was also concluded by (Vink & Kuiper 2006) for other SNRs hosting magnetars.

### 3.4. Can the Magnetar Contribute to TeV Emission?

HESS observations reported in Aharonian et al. (2008a) localized the TeV emission to the center of the radio shell of CTB 37B, and found that the extent of the TeV source is compatible with either a centrally peaked Gaussian of  $\sigma = 2'.6 \pm 0'.8$  or a shell of radius  $4'–6'$ , consistent with the size of the radio remnant. The energy flux of HESS J1713–381 from 0.2–10 TeV is  $\approx 4.2 \times 10^{-12} \text{ erg cm}^{-2} \text{ s}^{-1}$ , corresponding to luminosity  $L_\gamma = 3.2 \times 10^{34} \text{ d}_8^2 \text{ erg s}^{-1}$ , which we note is almost equal to the spin-down power of CXOU J171405.7–381031,  $\dot{E} = 4.2 \times 10^{34} \text{ erg s}^{-1}$ . Previous authors have argued that particles accelerated at the SNR shock are responsible for the TeV emission from HESS J1713–381 via pion decay (Aharonian et al. 2008a) or multi-zone inverse Compton scattering of the microwave background (Nakamura et al. 2009). As it is not clear if the TeV source has a pure shell-like morphology, it cannot be ruled out that the pulsar makes some contribution to the

TeV flux, possible via inverse Compton scattering from a PWN that is confined within the SNR shell.

Since the TeV luminosity of HESS J1713–381 is almost equal to the *present* spin-down power of CXOU J171405.7–381031, a scenario for a pulsar-powered TeV nebula would necessarily involve particles injected at an earlier time when its spin-down power was larger. However, unlike ordinary pulsars, it is not certain that magnetars can accelerate particles to TeV energies. Magnetar models that involve strong currents on closed, twisted magnetic field lines develop voltages of only  $\sim 10^9$  V (Beloborodov & Thompson 2007). On the other hand, it is not excluded that the ordinary pulsar mechanism operates on open magnetic field lines of magnetars, which may generate particle-dominated winds that become shocked PWNe, accelerating a fraction of the particles to TeV energies. Evidence for this possibility comes from the three magnetars that are also transient radio pulsars (Camilo et al. 2006, 2007; Levin et al. 2010). Even so, we caution that models for radio emission from magnetars (Thompson 2008a,b) produce average particle energies of only  $\sim 3$  GeV even on open field lines, because  $\gamma$ -rays make pairs more easily in the strong magnetic field.

Nevertheless, if high-energy electrons are generated in a shocked PWN in an early stage and escape the high  $B$ -field region, they can emit via inverse Compton scattering into the TeV band for an extended time (de Jager & Djannati-Ataï 2008). Electron lifetimes against synchrotron and inverse Compton losses are

$$t_s \approx \frac{4200 \text{ yr}}{\sqrt{E_\gamma(\text{TeV})}} \left( \frac{B}{10 \mu\text{G}} \right)^{-2}$$

and

$$t_{\text{IC}} \approx \frac{8 \times 10^4 \text{ yr}}{\sqrt{E_\gamma(\text{TeV})}},$$

respectively, for an electron producing a photon of energy  $E_\gamma(\text{TeV})$  by inverse Compton scattering of the microwave background. The limiting lifetime of such a relic nebula is then determined by  $t_s$  as long as  $B > 2 \mu\text{G}$ .

The spin-down power of CXOU J171405.7–381031 was certainly large enough to generate a TeV PWN during the history of CTB 37B, as long as it was born with a period significantly shorter than its present value, since  $\dot{E} = 9 \times 10^{36} P^{-4} (B_s/5 \times 10^{14} \text{ G})^2 \text{ erg s}^{-1}$ . The current TeV luminosity of HESS J1713–381,  $\approx 3.2 \times 10^{34} \text{ erg s}^{-1}$ , if radiated for 1000 yr, amounts to  $\sim 1 \times 10^{45} \text{ erg}$ , which is  $< 10^{-3}$  of the initial rotational energy of the pulsar for  $P_0 < 0.14$  s. Thus, we consider an inverse Compton PWN to be a plausible channel for TeV emission from CXOU J171405.7–381031 because it requires only a small fraction of the rotational energy to be deposited in very high-energy electrons.

A possible prototype of such systems is PSR J1846–0258, the “transitional”  $\sim 700$  yr old pulsar (Gotthelf et al. 2000) associated with HESS J1846–029 in the shell-like SNR Kes 75 (Djannati-Ataï 2008). This 0.32 s pulsar has a dipole field that approaches magnetar strength ( $B_s = 4.9 \times 10^{13} \text{ G}$ ) and displays AXP-like bursts (Gavriil et al. 2008); it is therefore likely of an intermediate class connecting the rotation-powered and the magnetar pulsars. It is also one of the most energetic

pulsars; its  $\dot{E} = 8.1 \times 10^{36} \text{ erg s}^{-1}$  is easily sufficient to power its X-ray PWN and the compact TeV emission of HESS J1846–029 (Djannati-Ataï 2008). However, Kes 75 differs from CTB 37B in that it contains a powerful X-ray PWN, while there is no evidence of an X-ray PWN in CTB 37B. Although these SNRs are of comparable age, any X-ray PWN in CTB 37B may have evolved a factor of 10 faster than the one in Kes 75, based on the scaling of pulsar  $\dot{E}$  with true age  $T$  such that  $T \propto B_s^{-1}$  for a given  $\dot{E}$ . The lifetime of a hypothetical rotation-powered X-ray PWN around a magnetar must be relatively brief. Interestingly, Vink & Bamba (2010) claim to have detected the first X-ray PWN around a magnetar in an archival *Chandra* observation of 1E 1547.0–5408, the magnetar of highest  $\dot{E}$ . Although this would be an important precedent, we hesitate to interpret it as such because we have not clearly confirmed its existence in those data.

Evidence to associate any other magnetar with TeV emission is sparse. The AXP 1E 1841–045 in SNR Kes 73 is located at the edge of HESS J1841–055 (Aharonian et al. 2008b), but this is not a likely association because the TeV emission is  $\approx 1^\circ$  in diameter and may conceivably have more than one source, as considered by Sguera et al. (2009). Moreover, it can be expected that any high-energy particles are still contained within the SNR shell, which is much smaller than the TeV source. Recently, an extended TeV source that surrounds the massive, young star cluster Westerlund 1 has also been reported by HESS (Ohm et al. 2009). It is possible that this source is associated with a young pulsar born in the cluster, the transient AXP CXO J164710.2–455216 (Muno et al. 2006), or its supernova remnant. Notably absent among the reported HESS sources is 1E 1547.0–5408, the magnetar of highest  $\dot{E}$  and a small characteristic age similar to CXOU J171405.7–381031. It would be interesting to target 1E 1547.0–5408 for a deep observation by HESS as a second test of whether a young magnetar can produce a TeV source.

#### 4. X-RAY TIMING OBSERVATION OF XMMU J173203.3–344518 IN HESS J1731–347

In Paper I, we also presented an analysis of the point source XMMU J173203.3–344518 in the SNR G353.6–0.7 that has been identified with the TeV source HESS J1731–347 (Aharonian et al. 2008b; Tian et al. 2008). We found only marginal evidence for a 1 s period in an *XMM-Newton* observation, which, in combination with the absence of strong evidence for variability did not allow us to definitively classify XMMU J173203.3–344518. Both a magnetar and a weakly magnetized central compact object (CCO) remained possibilities. The spectrum of XMMU J173203.3–344518 was best fitted by a two blackbody model, which is common to members of both classes.

We obtained a new *Chandra* observation of XMMU J173203.3–344518 on 2010 May 18 using ACIS-S in CC-mode for 40 ks. Using the same analysis techniques as described in Section 2 for CC-mode data, our period search of XMMU J173203.3–344518 did not reveal the candidate signal at 1 s, nor any other

TABLE 4  
*Chandra* OBSERVATION OF  
 XMMU J173203.3–344518 IN G353.6–0.7

Parameter	2010 May 18
ObsID	11234
Mode	ACIS-S3/CC/F
Exp. time (s)	39,920
Counts (s <sup>-1</sup> )	0.334
R.A. (J2000) <sup>a</sup>	17 <sup>h</sup> 32 <sup>m</sup> 03 <sup>s</sup> .40
Decl. (J2000) <sup>a</sup>	−34°45′16″.77
Two Blackbody Model	
$N_{\text{H}}$ (10 <sup>22</sup> cm <sup>-2</sup> )	2.13 <sup>+0.16</sup> <sub>-0.14</sub>
$kT_1$ (keV)	0.36 <sup>+0.04</sup> <sub>-0.05</sub>
$R_1$ (km)	2.1 <sup>+1.3</sup> <sub>-0.4</sub>
$kT_2$ (keV)	0.61 ± 0.07
$R_2$ (km)	0.44 <sup>+0.32</sup> <sub>-0.29</sub>
$F_x$ (0.5 – 10 keV) <sup>b</sup>	2.74 × 10 <sup>-12</sup>
$L_x$ (0.5 – 10 keV) <sup>c</sup>	1.26 × 10 <sup>34</sup>
$L_{\text{bol}}$ <sup>b</sup>	1.34 × 10 <sup>34</sup>
$\chi^2_\nu$	1.066(102)

<sup>a</sup> Measured from *Chandra* ACIS-I ObsID 9139. Typical *Chandra* ACIS coordinate uncertainty is 0′.6.

<sup>b</sup> Absorbed flux in units of erg cm<sup>-2</sup> s<sup>-1</sup>.

<sup>c</sup> Unabsorbed luminosity in units of erg s<sup>-1</sup>, assuming  $d = 3.2$  kpc.

significant period. The 95% confidence upper limit on the pulsed fraction of a sinusoidal signal is 8.6% for any period down to 10 ms. If restricted to periods  $\geq 1$  s, the corresponding limit is 7.6%. We also performed searches in restricted energy bands, in case there is a pulsation with an energy-dependent phase reversal similar to PSR J0821–4300 in Puppis A (Gotthelf & Halpern 2009), but no such signal was found.

We fitted the spectrum to a two blackbody model, which was the best fitting model to previous observations of XMMU J173203.3–344518 in Paper I. The result is shown in Figure 6; the data is grouped with 100 counts per bin. Table 4 gives the parameters of the two blackbody fit. These are consistent with the previous observations; in particular, the 0.5–10 keV flux is identical to that of an *XMM-Newton* observation from the year 2007 (Paper I). The absence of variability and pulsations tends to favor a CCO; several of the latter have very low limits on pulsed fraction (Halpern & Gotthelf 2010b, and references therein). If so, XMMU J173203.3–344518 would be the most luminous CCO, with  $L_x \approx 1 \times 10^{34}$  erg s<sup>-1</sup>. Recently, HESS was able to resolve the TeV emission of HESS J1731–347 into a shell that matches the size of the radio remnant G353.6–0.7 (Acero et al. 2009). This would tend to rule out the central source XMMU J173203.3–344518 as a source of the TeV emission.

## 5. CONCLUSIONS

In Paper I, we reported the discovery of the 3.82 s pulsar CXOU J171405.7–381031 in CTB 37B, which is coincident with the TeV source HESS J1713–381. Additional X-ray timing measurements reported here for the first time reveal the spin-down rate. CXOU J171405.7–381031 is one of the most energetic magnetars in terms of spin-down power, and has a characteristic timing age of  $\sim 1000$  years or less. Its

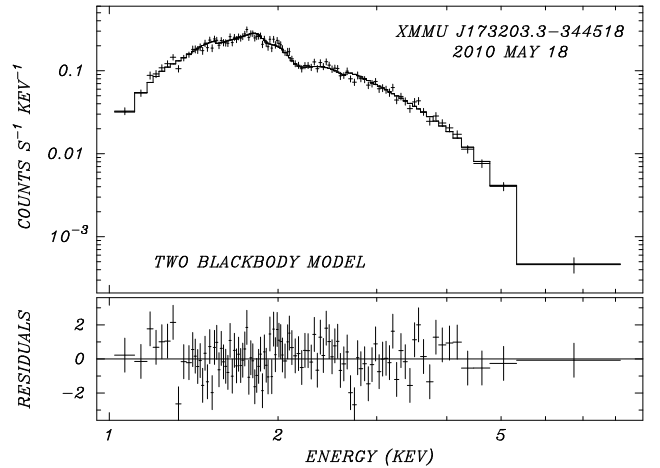


FIG. 6.— Spectrum of XMMU J173203.3–344518 in G353.6–0.7 from the *Chandra* ACIS-S3 CC-mode observation of 2010 May 18 fitted with two blackbodies. Fitted parameters are listed in Table 4.

timing age is roughly consistent with other estimates of the age of the SNR. In addition, there is some evidence for long-term variability by a factor of  $\sim 2$  in spin-down rate, which recently is found at its highest measured value. Its  $\dot{E}$  falls in the range occupied by SGRs, which may portend a future SGR outburst. The off-center location of the pulsar inside the SNR shell is probably a result of the inhomogeneous medium in which the shell expanded, rather than indicating an unprecedented high natal kick velocity.

There are considerable theoretical obstacles to getting particles of TeV energy from a magnetar, as well as having them emit primarily TeV  $\gamma$ -rays. As well, there is little observational evidence for such particles in the form of an X-ray synchrotron nebula. Nevertheless, the exceptional youth and high  $\dot{E}$  of CXOU J171405.7–381031 lead us to entertain the possibility that it generated a relic PWN that is now emitting primarily via inverse Compton scattering at TeV energies. Future imaging atmospheric Cherenkov observations to try to resolve the shell of CTB 37B from the pulsar could test this hypothesis.

Turning to another compact source in a HESS SNR, we obtained a second X-ray timing observation of XMMU J173203.3–344518 in HESS J1731–347/G353.6–0.7, but did not succeed in discovering a period. Its nature remains ambiguous because its composite spectrum, best fitted with two blackbodies, is characteristic of either AXPs or CCOs. In comparison with three previous X-ray observations of this source, the absence of obvious variability so far is consistent with XMMU J173203.3–344518 being a CCO (anti-magnetar). Deeper observations will be necessary to discover its timing properties, which would determine conclusively whether it is a magnetar or an anti-magnetar. The present upper limit on pulsed fraction is comparable to the weakest pulsations observed in magnetars including, at times, 1E 1547.0–5408 (Halpern et al. 2008), and similar to the upper limits on several CCOs (Halpern & Gotthelf 2010b) for which pulsations have not been detected. Even if pulsations are absent, continuing monitoring of XMMU J173203.3–344518 for variability may also



resolve its nature, since only a magnetar would be variable.

Support for this work was provided by the National Aeronautics and Space Administration through *Chan-*

*dra* Awards GO9-0063X and GO0-11085X issued by the *Chandra* X-ray Observatory Center, which is operated by the Smithsonian Astrophysical Observatory for and on behalf of NASA under contract NAS8-03060.

## REFERENCES

- Acero, F., Pühlhofer, G., Klochkov, D., Komin, Nu., Gallant, Y., & Horns, D., & Santangelo, A. 2009, in Proc. 31st Int. Cosmic Ray Conf. (Lodz), in press (arXiv:0907.0642)
- Aharonian, F., et al. 2006, ApJ, 636, 777
- Aharonian, F., et al. 2008a, A&A, 486, 829
- Aharonian, F., et al. 2008b, A&A, 477, 353
- Arnaud, K. A. 1996, in ASP Conf. Ser. 101, Astronomical Data Analysis Software and Systems V, ed. G. H. Jacoby & J. Barnes (San Francisco, CA: ASP), 17
- Arons, J. 2003, ApJ, 589, 871
- Beloborodov, A. M., & Thompson, C. 2007, ApJ, 657, 967
- Buccheri, R., et al. 1983, A&A, 128, 245
- Camilo, F., Ransom, S. M., Halpern, J. P., & Reynolds, J. 2007, ApJ, 666, L93
- Camilo, F., Ransom, S. M., Halpern, J. P., Reynolds, J., Helfand, D. J., Zimmerman, N., & Sarkissian, J. 2006, Nature, 442, 892
- Camilo, F., Reynolds, J., Johnston, S., Halpern, J. P., & Ransom, S. M. 2008, ApJ, 679, 681
- Carrigan, S., Hinton, J. A., Hofmann, W., Kosack, K., Lohse, T., & Reimer, O. 2008, in Proc. 30th Int. Cosmic Ray Conf. (Merida), 659
- Cassam-Chenaï, G., Decourchelle, A., Ballet, J., Sauvageot, J.-L., Dubner, G., & Giacani, E. 2004, A&A, 427, 199
- Clark, D. H., & Stephenson, F. R. 1975, The Observatory, 95, 190
- de Jager, O. C., & Djannati-Ataï, A. 2008, in Neutron Stars and Pulsars: 40 Years After Their Discovery, ed. W. Becker (Berlin: Springer), 451
- Djannati-Ataï, A. et al. 2008, in Proc. 30th Int. Cosmic Ray Conf., ed. R. Caballero, J. C. D’Olivo, G. Medina-Tanco, L. Nellen, F. A. Sánchez, J. F. Valdés-Galicia (Mexico City: Universidad Nacional Autónoma de México), 2, 823
- Esposito, P., et al. 2009, MNRAS, 399, L44
- Fernández, R., & Thompson, C. 2007, ApJ, 660, 615
- Gaensler, B. M., Slane, P. O., Gotthelf, E. V., & Vasisht, G. 2001, ApJ, 559, 963
- Gallant, Y. A., et al. 2008, in AIP Conf. Proc., Vol. 983, 40 Years of Pulsars: Millisecond Pulsars, Magnetars and More, ed. C. Bassa et al. (Melville, NY: AIP), 195
- Gavril, P. P., Gonzalez, M. E., Gotthelf, E. V., Kaspi, V. M., Livingstone, M. A., & Woods, P. M. 2008, Science, 319, 1802
- Gelfand, J. D., & Gaensler, B. M. 2007, ApJ, 667, 1111
- Gotthelf, E. V., & Halpern, J. P. 2009, ApJ, 695, L35
- Gotthelf, E. V., Vasisht, G., Boylan-Kolchin, M., & Torii, K. 2000, ApJ, 542, L37
- Green, D. A. 2009, Bull. Astron. Soc. India, 37, 45
- Halpern, J. P., & Gotthelf, E. V. 2010a, ApJ, 710, 941 (Paper I)
- Halpern, J. P., & Gotthelf, E. V. 2010b, ApJ, 709, 436
- Halpern, J. P., Gotthelf, E. V., Reynolds, J., Ransom, S. M. & Camilo, F. 2008, ApJ, 676, 1178
- Helfand, D. J., Chatterjee, S., Briskin, W. F., Camilo, F., Reynolds, J., van Kerkwijk, M. H., Halpern, J. P., & Ransom, S. M. 2007, ApJ, 662, 1198
- Hessels, J. W. T., et al. 2008, ApJ, 682, L41
- Kargaltsev, O., & Pavlov, G. G. 2010, in AIP Conf. Proc. 1248, X-ray Astronomy 2009: Present Status, Multi-wavelength Approach and Future Perspectives, ed. A. Comastri, L. Angelini, & M. Cappi (Melville, NY: AIP), 25
- Kassim, N. E., Baum, S. A., & Weiler, K. W. 1991, ApJ, 374, 212
- Lemière, A., Djannati, A., de Jager, O., & Terrier, R. 2008, in Proc. 30th Int. Cosmic Ray Conf. (Merida), 831
- Levin, L., et al. 2010, ApJ, 721, L33
- Mattana, F., et al. 2009, ApJ, 694, 12
- Muno, M. P., et al. 2006, ApJ, 636, L41
- Nakamura, R., Bamba, A., Ishida, M., Nakajima, H., Yamazaki, R., Terada, Y., Pühlhofer, G., & Wagner, S. J. 2009, PASJ, 61, S197
- Ohm, S., Horns, D., Reimer, O., Hinton, J., Rowell, G., de Oña Wilhelmi, E., Virgilio Fernandez, M., Acero, F., & Marcowith, A. 2009, in ASP Conf. Ser. 422, High-Energy Phenomena in Massive Stars, ed. J. Martí, P. L. Luque-Escamilla, & J. A. Combi (San Francisco, CA: ASP), 265
- Sato, T., Bamba, A., Nakamura, R., & Ishida, M. 2010, PASJ, in press (arXiv:1008.0234)
- Sguera, V., Romero, G. E., Bazzano, A., Masetti, N., Bird, A. J. & Bassani, L. 2009, ApJ, 697, 1194
- Strutt, J. W. 1880, Philos. Mag., 10, 73
- Sugizaki, M., Mitsuda, K., Kaneda, H., Matsuzaki, K., Yamauchi, S., & Koyama, K. 2001, ApJS, 134, 77
- Tanaka, Y., Inoue, H., & Holt, S. S. 1994, PASJ, 46, L37
- Thompson, C. 2008a, ApJ, 688, 1258
- Thompson, C. 2008b, ApJ, 688, 499
- Thompson, C., & Duncan, R. C. 1993, ApJ, 408, 194
- Tian, W. W., Leahy, D. A., Haverkorn, M., & Jiang, B. 2008, ApJ, 679, L85
- Vink, J., & Bamba, A. 2010, ApJ, 707, L148
- Vink, J., & Kuiper, L. 2006, MNRAS, 370, L14
- Wang, Z.-R. 2006, Ap&SS, 305, 207
- Wang, Z.-R., Qu, Q.-Y., & Chen, Y. 1997, A&A, 318, L59
- Woods, P. M., Kouveliotou, C., Finger, M. H., Göğüş, E., Wilson, C. A., Patel, S. K., Hurley, K., & Swank, J. H. 2007, ApJ, 654, 470
- Zhang, L., Chen, S. B., & Fang, J. 2008, ApJ, 676, 1210